Sensitivity of quantum gate fidelity to laser noise

X. Jiang, M. Friesen, and M. Saffman
Department of Physics, University of Wisconsin-Madison,
1150 University Avenue, Madison, Wisconsin 53706
(Dated: August 4, 2021)

If you want a good gate, better get a good laser.

CONTENTS

I. INTRODUCTION (MARK S)

♠ in progress

Logical gate operations on qubits rely on coherent driving with electromagnetic fields. For solid state qubits these are generally at microwave frequencies of 1-10 GHz. For atomic qubits both microwave and optical fields are used for gates. High fidelity gate operations require well controlled fields with very low amplitude and phase noise. In this paper we quantify the influence of control field noise on the fidelity of qubit control operations. While we mainly focus on the case of optical control with visible or infrared lasers, our results are also applicable to high fidelity control of solid state qubits, either superconducting or semiconductor based.

Although the limits imposed on gate fidelity by control field noise are of central importance in the quest for improving performance, the topic has received relatively little attention in the literature. The influence of laser noise on Rydberg gate fidelity was analyzed in [1]

II. LASER NOISE ANALYSIS

Rabi oscillations of a qubit are driven by a laser, whose complex representation is given by

$$\mathbf{E}(t) = \hat{e}E_0 \exp[i(2\pi\nu t + \phi(t))]. \tag{1}$$

Fluctuations of this laser field represent one of the main sources of qubit decoherence, and may occur in the polarization $\hat{e}$, the amplitude E_0, or the phase ϕ parameters. For the lasers of interest in many recent qubit experiments, the predominant fluctuations occur in the phase variable. In this work, we therefore simply ignore the polarization and amplitude fluctuations to focus on the fluctuations of $\phi(t)$. Alternatively, and equivalently, we may consider fluctuations of the frequency, $\nu(t) = \nu_0 + \delta\nu(t)$, which are related to phase fluctuations through the relation

$$\phi(t) = \int_{t_0}^{t_0+t} 2\pi\delta\nu(t')dt', \tag{2}$$

where t_0 is a reference time.

The fluctuations of $\delta\nu(t)$ [or $\phi(t)$] have a direct influence on the Rabi oscillations, and must therefore be carefully characterized. A compact description of a general fluctuating variable $X(t)$ is given by its autocorrelation function, defined as

$$R_X(\tau) = \langle X(t)X(t+\tau)\rangle \equiv \lim_{T\to\infty}\frac{1}{2T}\int_{-T}^{T} X(t)X(t+\tau)dt. \tag{3}$$

According to the Weiner-Khintchine theorem, the autocorrelation function of $X(t)$ is related to its noise power spectrum by the Fourier transform,

$$S_X(f) = \int_{-\infty}^{\infty} R_X(\tau)e^{-i2\pi f\tau}d\tau, \tag{4}$$

and its inverse transform,

$$R_X(\tau) = \int_{-\infty}^{\infty} S_X(f)e^{i2\pi f\tau}df, \tag{5}$$

where in this work, we consider two-sided power spectra.

The main goal of this work is to characterize the noise spectrum of $E(t)$. However, $S_E(f)$ (also called the laser lineshape) cannot be measured directly, due to the high frequency of the carrier. We must therefore transduce the power spectrum to lower frequencies. Here, we consider the self-heterodyne transduction technique, in which the laser field is split, modified, and recombined to perform interferometry measurements. The resulting signal is read out as a photocurrent containing a direct imprint of the underlying noise spectrum. For the dimensionless photocurrent $i(t)$, which we define below, the self-heterodyne power spectrum is denoted $S_i(f)$.

In this section, we derive the interrelated power spectra of $S_E(f)$ and $S_i(f)$, which are in turn functions of the underlying noise spectrum $S_{\delta\nu}(f)$ [or $S_\phi(f)$]. To perform noisy gate simulations, as discussed in later sections, one would like to use actual self-heterodyne experimental data to characterize the underlying noise spectra. In principle, such a deconvolution cannot be implemented exactly [2]. However, we will show that reliable results for the noise power may indeed be obtained, particularly for lasers with very low noise levels, such as the locked and filtered lasers used in recent qubit experiments.

A. Laser Lineshape

In Eq. (1), we employed a complex representation for the laser field. However, classical fields are real, and the corresponding autocorrelation function is defined as

$$R_E(\tau) = \langle E^*(t)E(t+\tau)\rangle. \tag{6}$$

This function contains information about both the carrier signal, centered at frequency ν_0, and the fluctuations, which are typically observed as a fundamental broadening of the carrier peak. Additional features of importance for qubit experiments include structures away from the peak that may be caused by the laser locking and filtering circuitry, such as the "servo bump," discussed in detail below.

The time average in Eq. (6) has been evaluated by a number of authors. We summarize these derivations here, for completeness, following the approach of Ref. [3]. From Eqs. (1) and (6), we obtain

$$R_E(\tau) = E_0^2 e^{i2\pi\nu_0\tau}\langle e^{i[\phi(t+\tau)-\phi(t)]}\rangle. \tag{7}$$

To begin, we assume the noise process is strongly stationary, so that $\langle\phi(t)\phi(t+\tau)\rangle$ does not depend on t. We then assume that the phase difference, $\Phi(\tau) \equiv \phi(t+\tau)-\phi(t)$, is a gaussian random variable centered at $\Phi(\tau) = 0$, with the probability distribution

$$p(\Phi) = \frac{1}{\sigma_\Phi\sqrt{2\pi}} e^{-\Phi^2/2\sigma_\Phi^2},$$

and variance $\overline{\Phi^2} = \sigma_\Phi^2$, where the bar denotes an ensemble average. According to the ergodic theorem, the ensemble and time averages must be equivalent, so that

$$\sigma_\Phi^2(\tau) = \langle[\phi(t+\tau)-\phi(t)]^2\rangle = 2R_\phi(0) - 2R_\phi(\tau), \tag{8}$$

where we note that

$$\langle\phi^2(t)\rangle = \langle\phi^2(t+\tau)\rangle = R_\phi(0).$$

Again, making use of the ergodic theorem, we have

$$\langle e^{i\Phi}\rangle = e^{-\sigma_\Phi^2/2}, \tag{9}$$

which is also known as the moment theorem for gaussian random variables. Combining Eqs. (7)-(9), we obtain the important relation [4]

$$R_E(\tau) = E_0^2 e^{i2\pi\nu_0\tau}\exp\left[R_\phi(\tau) - R_\phi(0)\right]. \tag{10}$$

Note that since ϕ can take any value, $R_\phi(0)$ does not have physical significance on its own; only the difference $R_\phi(\tau) - R_\phi(0)$ is meaningful.

Another useful form for Eq. (10) can be obtained from the relation $2\pi\delta\nu(t) = \partial\phi/\partial t$, together with Eq. (4) and the stationarity of $R_\phi(t)$, yielding

$$S_{\delta\nu}(f) = f^2 S_\phi(f). \tag{11}$$

Applying trigonometric identities, we then obtain the following, well-known results for the laser lineshape [2]:

$$R_E(\tau) = E_0^2 e^{i2\pi\nu_0\tau}\exp\left[-2\int_{-\infty}^{\infty} S_{\delta\nu}(f)\frac{\sin^2(\pi f\tau)}{f^2}\,df\right], \tag{12}$$

and

$$S_E(f) = E_0^2\int_{-\infty}^{\infty}\cos[2\pi(f-\nu_0)\tau]\exp\left[-2\int_{-\infty}^{\infty} S_{\delta\nu}(f')\frac{\sin^2(\pi f'\tau)}{(f')^2}\,df'\right]d\tau. \tag{13}$$

It is common to adopt a lineshape that is centered at zero frequency; henceforth, we therefore set $\nu_0 = 0$.

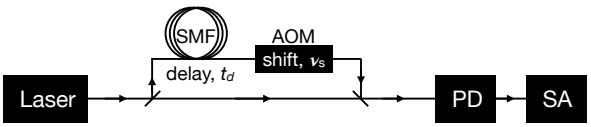

FIG. 1. Heterodyne setup. The laser signal is split equally between two paths. One path passes through a single-mode fiber (SMF), where it is delayed by time t_d. It then also passes through an acousto-optic modulator (AOM), where its frequency is shifted by ν_s. The beams are then recombined and measured by a photodiode (PD), and the signal is processed by a spectrum analyzer (SA).

We note that $S_E(f)$ is properly normalized here, with $\int_{-\infty}^{\infty} S_E(f)df = E_0^2$. Thus, fluctuations that broaden the lineshape also reduce the peak height.

Some additional interesting results follow from Eq. (13). First, in the absence of noise [$S_{\delta\nu} = 0$], we see that the laser lineshape immediately reduces to an unbroadened carrier signal: $S_E(f) = E_0^2\delta(f)$. Second, when $S_{\delta\nu}$ is nonzero but small, as typical for a locked and filtered laser, the exponential term in Eq. (13) may be expanded to first order, yielding [5]

$$S_E(f)/E_0^2 \approx [1 - R_\phi(0)]\delta(f) + S_\phi(f). \tag{14}$$

This approximation is generally very good, but breaks down in the asymptotic limit $\tau \to \infty$ of the τ integral, and therefore the limit $f \to 0$. To see this, we note that $\sin^2(\pi f\tau)$ may be replaced by its average value of $1/2$ in the integral; for nonvanishing values of $S_{\delta\nu}(0)$, the argument of the exponential then diverges. To estimate the frequency f_x, below which Eq. (14) breaks down, we set the argument of the exponential to $1/2$:

$$2\int_{f_x}^{\infty} \frac{S_{\delta\nu}(f)}{f^2}df \approx \frac{1}{2}. \tag{15}$$

This criterion clearly depends on the noise spectrum.

To conclude, we note that for some analytical calculations (such as the servo-bump analysis, described below), it may be convenient to separate the noise spectrum into distinct components: $S_{\delta\nu}(f) = S_{\delta\nu,1}(f) + S_{\delta\nu,2}(f)$. The resulting lineshapes can then be written as

$$R_E(\tau) = E_0^{-2} R_{E,1}(\tau) R_{E,2}(\tau), \tag{16}$$

where $R_{E,1}(\tau)$ and $R_{E,2}(\tau)$ are the autocorrelation functions corresponding to $S_{\delta\nu,1}(f)$ and $S_{\delta\nu,2}(f)$. Applying the Fourier convolution theorem, we obtain

$$S_E(f) = E_0^{-2}\int_{-\infty}^{\infty} S_{E,1}(f - f')S_{E,2}(f')df'. \tag{17}$$

B. Self-Heterodyne Spectrum

We consider the self-heterodyne optical circuit shown in Fig. 1. As depicted in the diagram, one of the paths is delayed by time t_d, through a long optical fiber, and then shifted in frequency by ν_s, by means of an acousto-optic modulator. Here, the delay loop allows us to interfere phases at different times, while the frequency shift provides a beat tone that is readily accessible to electronic measurements, since it occurs at submicrowave frequencies, $\nu_s \approx 100$ MHz. The two beams are then recombined and the total intensity is measured by a photodiode, using conventional measurement techniques.

For simplicity, we assume the laser signal is split equally between the two paths, although unequal splitting may also be of interest [6]. The recombined field is given by

$$\begin{aligned} E(t) &= E_0 \exp[i(2\pi\nu_0 t + \phi(t))] \\ &+ E_0 \exp[i2\pi\nu_0(t - t_d) + i\phi(t - t_d) + i2\pi\nu_s(t - t_d)]. \end{aligned} \tag{18}$$

The output of the photodiode is then proportional to

$$I(t) \sim E^*(t)E(t). \tag{19}$$

For convenience, we consider instead a dimensionless photocurrent $i(t)$, consistent with Eq. (19), given by

$$i(t) = 2 + 2\cos[2\pi\nu_0 t_d - 2\pi\nu_s(t - t_d) + \phi(t) - \phi(t - t_d)], \tag{20}$$

where the factors of 2 will be explained shortly. The corresponding autocorrelation function is given by

$$R_i(\tau) = \langle i(t)i(t + \tau)\rangle. \tag{21}$$

The evaluation of $R_i(\tau)$ is simplified by noting that terms proportional to t inside the cosine functions cause those functions to average to zero. We then obtain

$$\begin{aligned} &R_i(\tau) = 4 \\ &+2\langle\cos[2\pi\nu_s\tau+\phi(t)-\phi(t-t_d)-\phi(t+\tau)+\phi(t+\tau-t_d)]\rangle. \end{aligned} \tag{22}$$

Now, following the derivation of $R_E(\tau)$, we assume that $\Phi' = \phi(t) - \phi(t - t_d) - \phi(t + \tau) + \phi(t + \tau - t_d)$ is a gaussian random variable centered at zero, and we apply the gaussian moment relations,

$$\langle\cos(\Phi')\rangle = e^{-\sigma_{\Phi'}^2/2} \quad \text{and} \quad \langle\sin(\Phi')\rangle = 0, \tag{23}$$

where

$$\sigma_{\Phi'}^2 = \langle[\phi(t)-\phi(t-t_d)-\phi(t+\tau)+\phi(t+\tau-t_d)]^2\rangle, \tag{24}$$

to obtain

$$\begin{aligned} R_i(\tau) &= 4 + 2\cos(2\pi\nu_s\tau) \\ &\times \exp[2R_\phi(\tau) + 2R_\phi(t_d) - 2R_\phi(0) \\ &- R_\phi(\tau - t_d) - R_\phi(\tau + t_d)]. \end{aligned} \tag{25}$$

Here, the cosine function describes the beat tone, and the noise information is reflected in its amplitude. It can

be seen that the corresponding power spectrum, $S_i(f)$, includes a central peak, $\delta(f)$, which contains no information about the laser noise, and two broadened and identical satellite peaks, centered at $f = \pm\nu_s$. We now redefine $R_i(\tau)$ to be consistent with typical self-heterodyne measurements, which are recentered at one of the satellite peaks, such that

$$R_i(\tau) \to \tilde{R}_i(\tau) = \exp[2R_\phi(\tau) + 2R_\phi(t_d) - 2R_\phi(0) - R_\phi(\tau - t_d) - R_\phi(\tau + t_d)]. \quad (26)$$

Henceforth, we simply drop the tilde notation. Applying trigonometric identities, we then obtain

$$R_i(\tau) = \exp\left[-8\int_{-\infty}^{\infty} S_{\delta\nu}(f)\frac{\sin^2(\pi f\tau)\sin^2(\pi f t_d)}{f^2}df\right], \quad (27)$$

and

$$S_i(f) = \int_{-\infty}^{\infty} \cos(2\pi f\tau)R_i(\tau). \quad (28)$$

Here we note that the self-heterodyne peak is properly normalized, with $\int_{-\infty}^{\infty} S_i(f)df = R_i(0) = 1$, which explains our normalization choice in Eq. (20).

In the absence of noise [$S_{\delta\nu} = 0$], we see from Eqs. (27) and (28) that the self-heterodyne power spectrum reduces to the bare carrier: $S_i(f) = \delta(f)$. For nonzero but small $S_{\delta\nu}$, we can expand the exponential in Eq. (27), as we did in Eq. (14), to obtain

$$S_i(f) \approx \left[1 + 2R_\phi(t_d) - 2R_\phi(0)\right]\delta(f) + 4\sin^2[\pi f t_d]S_\phi(f). \quad (29)$$

As before, this expansion breaks down at low frequencies. However, the well-known "scallop" features in the power spectrum are readily apparent, arising from the $\sin^2[\pi f t_d]$ factor in Eq. (**??**). This result immediately demonstrates the ability of the self-heterodyne technique to probe the underlying laser noise, and moreover, to predict the laser lineshape:

$$E_0^2 S_i(f) \approx 4S_E(f)\sin^2(\pi f t_d), \quad (30)$$

where here, we ignore the central carrier peaks.

To conclude, we again consider the possibility that the noise spectrum may be separated into distinct components, $S_{\delta\nu}(f) = S_{\delta\nu,1}(f) + S_{\delta\nu,2}(f)$. As for the laser lineshape, the self-heterdyne autocorrelation function may then be written as

$$R_i(\tau) = R_{i,1}(\tau)R_{i,2}(\tau), \quad (31)$$

yielding the combined power spectrum

$$S_i(f) = \int_{-\infty}^{\infty} S_{i,1}(f - f')S_{i,2}(f')df'. \quad (32)$$

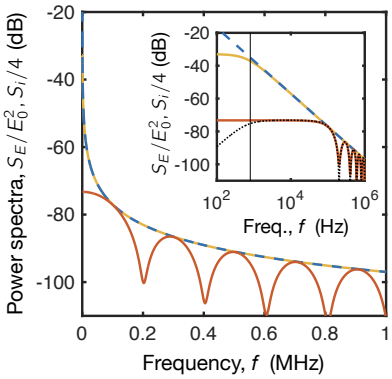

FIG. 2. White noise power spectra. $S_E(f)/E_0^2$, from Eq. (36)], is plotted as gold. $S_i(f)/4$, from Eq. (39), is plotted as red. We also plot $S_\phi(f)$ (dashed blue), which provides a very good approximation for $S_E(f)$ when $S_\phi(f)$ is small [see Eq. (14)]. Inset: Same quantities, plotted on a logarighmic frequency scale. Here we also plot the cutoff frequency f_x as a vertical black line, below which Eq. (14) breaks down, and we plot the approximate form for $S_i(f)/4$ from Eq. (29), which also breaks down at low frequencies.

C. White Noise

The self-heterodyne laser noise measurements, reported below, appear to be well described by a combination of white noise in $S_{\delta\nu}$, and a Gaussian servo-bump noise model. We now obtain analytical results for the $S_E(f)$ and $S_i(f)$ power spectra, for these two noise models. The power spectra for white noise are well-known [7]. However we include them here for completeness.

The underlying noise spectrum for white noise is given by

$$S_{\delta\nu} = h_0 \qquad \text{or} \qquad S_\phi(f) = \frac{h_0}{f^2}. \quad (33)$$

Note that it is common to use a one-sided noise spectrum for such calculations; however we use a two-sided spectrum here. Our results may therefore differ by a factor of 2 from others reported in the literature. The most straightforward calculation of $R_\phi(\tau)$, from Eq. (33), immediately encounters a singularity. We therefore proceed by calculating $R_E(\tau)$ from Eq. (12). Setting $\nu_0 = 0$, to center the power spectrum, then gives

$$R_E(\tau) = E_0^2 e^{-2\pi^2 h_0|\tau|}. \quad (34)$$

From Eq. (10), we can identify

$$R_\phi(\tau) - R_\phi(0) = -2\pi^2 h_0|\tau|, \quad (35)$$

where the singularity has now been absorbed into $R_\phi(0)$. Solving for the laser lineshape yields

$$S_E(f) = \frac{E_0^2 h_0}{f^2 + (\pi h_0)^2}, \quad (36)$$

for which the FWHM linewidth is $2\pi h_0$. Away from the carrier peak, which is very narrow for a locked and well-filtered laser, we find

$$S_E(f)/E_0^2 \approx \frac{h_0}{f^2} = S_\phi(f), \tag{37}$$

as consistent with Eq. (14). Equations (36) and (37) are plotted in Fig. 2, in the form $S_E(f)/E_0^2$, demonstrating the accuracy of our approximations. Here, $S_E(f)$ is plotted in gold and $S_\phi(f)$ is plotted in dashed blue. The crossover frequency f_x [Eq. (15)], below which Eq. (37) breaks down, can be evaluated analytically for the case of white noise, giving $f_x = 4h_0$. This crossover is shown as a vertical black line in the inset of Fig. 2, where the same curves are plotted on a logarithmic frequency scale.

We can also evaluate the self-heterodyne autocorrelation function, Eq. (26), obtaining

$$R_i(\tau) = \exp\left[-2\pi^2 h_0(2t_d + 2|\tau| - |\tau - t_d| - |\tau + t_d|\right], \tag{38}$$

and the corresponding power spectrum,

$$S_i(f) = \frac{2h_0}{f^2 + (2\pi h_0)^2} + e^{-4\pi^2 h_0 t_d}\left\{\delta(f) - \frac{2h_0}{f^2 + (2\pi h_0)^2}\left[\cos(2\pi f t_d) + \frac{2\pi h_0}{f}\sin(2\pi f t_d)\right]\right\}. \tag{39}$$

In Fig. 2, we plot $S_i(f)/4$ with red lines, and in the inset, we also plot the approximate form for $S_i(f)/4$, from Eq. (29), as a dotted black line. Deviations between the exact and approximate forms for $S_i(f)$ are mainly observed at very low frequencies. We note that the delta function in Eq. (39) would normally be broadened by the measurement circuitry in real experiments; however we have not included such broadening here.

The scallop features in Fig. 2 are caused by the interfering fields of the self-heterodyne circuit. In principle, any fine-scale noise features present in $S_\phi(f)$ or $S_E(f)$ can also be seen in $S_i(f)$. However the fine features are obscured by the scallops, which suppress the measured signal at frequency intervals of $\Delta f = 1/t_d$.

D. Servo Bump

A laser can be stabilized by locking it to a narrow-linewidth reference cavity. This feedback system is called a servo loop [5], and the finite bandwidth of the feedback loop induces peaks in $S_{\delta\nu}(f)$ called a servo bumps, which are typically shifted to the left and right of the central peak by frequencies on the order of 1 MHz. We find that experimental servo bumps have approximately gaussian shapes. In fact, we find that the full noise model is well described by a gaussian servo bump combined with white noise, as defined by

$$\begin{aligned} S_{\delta\nu}(f) &= h_0 + h_g \exp\left[-\frac{(f-f_g)^2}{2\sigma_g^2}\right] + h_g \exp\left[-\frac{(f+f_g)^2}{2\sigma_g^2}\right] \\ &= h_0 + \frac{s_g f_g^2}{\sqrt{8\pi}\sigma_g}\exp\left[-\frac{(f-f_g)^2}{2\sigma_g^2}\right] + \frac{s_g f_g^2}{\sqrt{8\pi}\sigma_g}\exp\left[-\frac{(f+f_g)^2}{2\sigma_g^2}\right]. \end{aligned} \tag{40}$$

Here, h_g is the bump's height and σ_g is its width, with a FWHM given by $\sqrt{\ln 4}\,\sigma_g$.

In the second line of Eq. (40), we use an alternative expression for the bump height, in terms of its total, dimensionless phase-noise power, $s_g = \int_{-\infty}^{\infty} S_{\phi,g}(f)df$, where the subscript g refers to the gaussian noise components. We use this expression in the simulations described below, to explore the effects of different bump shapes. To perform the s_g conversion here, we note that $S_{\phi,g}(f)$ is actually singular at $f = 0$, causing its integral to diverge. We can regularize this divergence by assuming that the servo bump is narrow (which appears to be true in many experiments), and by making the substitution

$$S_\phi(f) = S_{\delta\nu}(f)/f^2 \approx S_{\delta\nu}(f)/f_g^2, \tag{41}$$

yielding $s_g \approx \sqrt{8\pi}\sigma_g h_g/f_g^2$, which is the form used in Eq. (40). We can think of this expression as describing the noise power in just the servo bump, and not the low-frequency portion of the spectrum. We emphasize that the latter is not ignored – but it is subsumed into the white noise, which we treat separately.

We first consider just the gaussian term in Eq. (40), setting $h_0 = 0$. Fourier transforming Eq. (41), we obtain

$$R_\phi(\tau) \approx s_g \cos(2\pi f_g \tau) e^{-2\pi^2\sigma_g^2\tau^2}. \tag{42}$$

Thus for $s_g \ll 1$, Eq. (14) gives

$$S_E(f)/E_0^2 \approx \delta(f) + \frac{h_g}{f_g^2}\exp\left[-\frac{(f-f_g)^2}{2\sigma_g^2}\right] + \frac{h_g}{f_g^2}\exp\left[-\frac{(f+f_g)^2}{2\sigma_g^2}\right], \tag{43}$$

and Eq. (29) gives

$$S_i(f) \approx \delta(f) + \frac{4h_g}{f_g^2}\sin^2(\pi f t_d)\exp\left[-\frac{(f-f_g)^2}{2\sigma_g^2}\right] + \frac{4h_g}{f_g^2}\sin^2(\pi f t_d)\exp\left[-\frac{(f+f_g)^2}{2\sigma_g^2}\right]. \quad (44)$$

The white noise component of $S_{\delta\nu}(f)$ can now be included, obtaining Eqs. (17) and (32), yielding

$$S_E(f) = E_0^{-2}\int_{-\infty}^{\infty} S_{E,w}(f-f')S_{E,g}(f')df', \quad (45)$$

$$S_i(f) = \int_{-\infty}^{\infty} S_{i,w}(f-f')S_{i,g}(f')df', \quad (46)$$

where the subscripts w and g refer to white and gaussian power spectra, which have already been computed. We solve these integrals, approximately, by noting that a convolution between two peaks, with very different widths, is dominated by the wider peak. We further note that, for the lasers of interest here, the servo bump is much wider than the white-noise Lorentzian peak, which is in turn much wider than a delta function. Hence, we find that

$$S_E(f)/E_0^2 \approx \frac{h_0}{f^2+(\pi h_0)^2} + \frac{h_g}{f_g^2}\exp\left[-\frac{(f-f_g)^2}{2\sigma_g^2}\right] + \frac{h_g}{f_g^2}\exp\left[-\frac{(f+f_g)^2}{2\sigma_g^2}\right], \quad (47)$$

and

$$S_i(f) \approx \frac{2h_0}{f^2+(2\pi h_0)^2} + e^{-4\pi^2 h_0 t_d}\left\{\delta(f) - \frac{2h_0}{f^2+(2\pi h_0)^2}\left[\cos(2\pi f t_d) + \frac{2\pi h_0}{f}\sin(2\pi f t_d)\right]\right\} + \frac{4h_g}{f_g^2}\sin^2(\pi f t_d)\exp\left[-\frac{(f-f_g)^2}{2\sigma_g^2}\right] + \frac{4h_g}{f_g^2}\sin^2(\pi f t_d)\exp\left[-\frac{(f+f_g)^2}{2\sigma_g^2}\right]. \quad (48)$$

In the following section, we apply these equations as fitting forms for experimental self-heterodyne data.

III. LASER CHARACTERIZATION (MARK F)

A. Ti:Sa laser

B. Diode laser

IV. RABI OSCILLATIONS WITH NOISY DRIVE (XIAOYU)

A. Dynamical equations

Two start with, we study a two-level system interacting with a monochromatic field. By writing the state of the system to be $|\psi\rangle = c_g(t)e^{-i\omega_g t}|g\rangle + c_e(t)e^{-i\omega_e t}|e\rangle$, and the electric field to be $E = (\varepsilon/2)e^{-i\omega t} + c.c.$, we can solve the Schrödinger equations directly and get the following dynamical equations:

$$\frac{d}{dt}c_g(t) = i\frac{\Omega_0}{2}e^{-i\Delta t}c_e(t) \quad (49)$$

$$\frac{d}{dt}c_e(t) = i\frac{\Omega_0^*}{2}e^{i\Delta t}c_g(t) \quad (50)$$

where Δ is the detuning $\Delta = \omega - \omega_{eg} = \omega - (\omega_e - \omega_g)$, and Ω_0 is the complex Rabi frequency $\Omega_0 = d_{eg}/\hbar$, where d_{eg} is the atomic diople moment.

For simplicity, we first assume that there are no detunings so that $\Delta = 0$. Then we can study how phase and intensity noise can affect the above dynamical equations. A time varying phase noise $\phi(t)$ gives an extra phase term $e^{i\phi(t)}$ to the right side of equation (1) and (2). For intensity noise, we use the following form:

$$I(t) = I_0 + \delta I(t) == I_0(1+\alpha_I(t)) \quad (51)$$

where I_0 is the intensity of the noise-free laser. We use $\alpha_I(t)$ to represent the time-varying relative intensity fluctuation. With these two types of time-varying noise, the dynamical equations become:

$$\frac{d}{dt}c_g(t) = i\frac{\Omega_0\sqrt{1+\alpha_I(t)}}{2}e^{i\phi(t)}c_e(t) \quad (52)$$

$$\frac{d}{dt}c_e(t) = i\frac{\Omega_0^*\sqrt{1+\alpha_I(t)}}{2}e^{-i\phi(t)}c_g(t) \quad (53)$$

This means we can simulate the response of the system with a 3-step recipe:First, calculate the noise spectrum of the laser of interest from lab self-heterodyne measurements, as we have already introduced in part II and III; Second, create samples of the time-varying noises $\alpha_I(t)$ and $\phi(t)$ from the noise spectrum; And last, we can plug $\alpha_I(t)$ and $\phi(t)$ into equations above and simulate the result with computer programs.

B. Time series reconstruction

This section introduces our method for creating noisy time series. Consider a random process $X(t)$ with power spectral density $S_X(f)$. One way to construct a sample of $\{X(t)\}$ is to use the deterministic amplitude scheme(DAS) mentioned in [**?**]. The recipe is as follows:

1. For a continuous $S_X^C(f)$, the power of $X(t)$ in frequency band f_1 and $f_2 > f_1$ can be calculated by the following integral:

$$P_{f_1<f<f_2} = \int_{f_1}^{f_2} S_X^C(f)df \quad (54)$$

which is a general property of random processes.

we can make $S_X^C(f)$ discrete by sampling it at frequency $f_k = k\Delta f$. Then for each f_k, the value of the discretized $S_X^D(f_k)$ should be the power contained in the band $[f_k, f_k + \Delta f]$, as we learned in section 1.1 and equation(11). We can get:

$$S_X^D(f_k) = S_X^C(f_k)\Delta f \tag{55}$$

Also please note we are using $S_X^C(f)$ as a one-sided power spectral density. This is also true for the rest part of the recipe.

2. Noticing that for a time series $X(t)$, it forms a Fourier pair with the amplitude spectrum $A_X(f_k)$. For a discretized signal, there is a simple relation between the power spectrum and the amplitude spectrum:

$$|A_X(f_k)| = \sqrt{|S_X^D|} = \sqrt{S_X^C(f_k)\Delta f} \tag{56}$$

3. Do a inverse discrete Fourier transform(IDFT) on the amplitude spectrum $A_X(f_k)$ to get a time series. Since S_X^C is real and even we can use a real Fourier tranform pair:

$$X(t_j) = \sum_k \sqrt{S_X^C(f_k)\Delta f}\cos(2\pi f_k t_j + \psi_k) \tag{57}$$

Here ψ_k is randomly chosen from a uniform distribution of $[0, 2\pi]$, j range from 1 to N, k range from 1 to $N/2$, where N is the sampling number, $t_k = k\Delta t$, and by Nyquist sampling theorem, $\Delta t = 1/(N\Delta k)$.

Equation (18) has a factor of 2 difference compared with the expression in [**?**]. This is because we are using a 1-sided power spectral density here.

One concern here is how we should assign the sampling interval Δk for $S_X^C(k)$. In principle, we think a larger k will give a more precise result, since we are approximating the integral in equation (6) to the area of the column in equation (7). Simulation results show that for $\Omega_0 = 1MHz$ and a white noise with bandwidth=10MHz, sample points larger than 1000 would give enough accuracy to the simulations result.

C. Numerical results

1. *One-photon transitions*

2. *Two-photon transitions*

V. QUASI-STATIC APPROXIMATIONS (XIAOYU)

For phase noise and intensity noise, we can try to use this quasi-static model to get an estimate of the population error.

In this section we only focus on noise spectrum with constant amplitude h and cut-off frequency $_c$. The other quantities that are important here are the Rabi frequency Ω_0, and the laser's full width at half maximum(FWHM) linewidth which are usually measured in self-heterodyne measurements in labs.

The first assumption we make here came from the study on the laser noise spectrum by Domenico et al. in 2010[**?**], where it was showed that, for a noise spectrum with constant amplitude h and cut-off frequency f_c, when condition $f_c > 1.78h$ is satisfied, the corresponding lineshape of the laser $S_E(\nu)$ is approximately Lorentzian, which gives a simple relation between FWHM and h:

$$h = \frac{FWHM}{h} \tag{58}$$

The second assumption is that when the bandwith of the noise spectrum is much less than the Rabi frequency, we can consider the noise to be quasi-static. We can treat the noise as a simple random variable instead of a random process.

A. Intensity Noise

Assume the output of a laser with intensity noise follows the following form:

$$I = I_0(1 + x) \tag{59}$$

where I_0 is the unperturbed intensity, x is the relative intensity noise.

Assume that x follows normal distribution with zero mean and variance σ:

$$f(x) = \frac{1}{\sqrt{2\pi}\sigma}e^{-\frac{x^2}{2\sigma^2}} \tag{60}$$

Here σ is the root-mean-square(RMS) intensity noise, which is the RIN level that we measure in labs.

Under this situation, the Rabi frequency for a two level system is then:

$$\Omega = \Omega_0\sqrt{1 + x} \tag{61}$$

where Ω_0 is the Rabi frequency when the intensity noise does not exist. Here to make the expression valid we need $-1 \le x \le 1$, which means the intensity noise is not greater than the signal.

Under the setting that $-1 \le x \le 1$, we need to modify the distribution of x to be a truncated-Gaussian:

$$f(x) = \begin{cases} \frac{1}{\sqrt{2\pi}\sigma \mathbf{Erf}(\frac{1}{\sqrt{2}\sigma})}e^{-\frac{x^2}{2\sigma^2}}, & \text{if } -1 \le x \le 1 \\ 0, & \text{otherwise} \end{cases}$$

In resonant Rabi oscillation the population probability for the ground state $|g\rangle$ is:

$$P_g = \cos^2(\frac{\Omega t}{2}) \tag{62}$$

Suppose we are interested on the expectation value of P_e after N cycles driven by a laser with intensity noise, $t_N = N\frac{2\pi}{\Omega_0}$. Then the expected value of P_e can be calculated by the following integral:

$$\mathrm{E}[P_g] = \frac{1}{\sqrt{2\pi}\sigma\mathbf{Erf}(\frac{1}{\sqrt{2}\sigma})}\int_{-1}^{1}\cos^2(\frac{\Omega t_N}{2})e^{-\frac{x^2}{2\sigma^2}}dx \quad (63)$$

$$= \frac{1}{\sqrt{2\pi}\sigma\mathbf{Erf}(\frac{1}{\sqrt{2}\sigma})}\int_{-1}^{1}\cos^2(N\pi\sqrt{1+x})e^{-\frac{x^2}{2\sigma^2}}dx \quad (64)$$

By assuming that x is very small, and doing Talor expansion on the cosine part of the integral, we get the following approximation to second order:

$$\cos^2(N\pi\sqrt{1+x}) \approx 1 - \frac{N^2\pi^2x^2}{4} \quad (65)$$

By plugging the approximation back and doing Gaussian integral on x between -1 and 1, we get:

$$\mathrm{E}[P_g] = 1 - \frac{N^2\pi^2\sigma^2}{4} + \frac{N^2\pi^{\frac{3}{2}}}{2\sqrt{2}}\frac{\sigma e^{-\frac{1}{2\sigma^2}}}{\mathbf{Erf}(\frac{1}{\sqrt{2}\sigma})} \quad (66)$$

The last term, with a $e^{-\frac{1}{2\sigma^2}}$ term, is zero in many orders of expansion. A good approximation will then be:

$$\mathrm{E}[P_g] = 1 - \frac{N^2\pi^2\sigma^2}{4} \quad (67)$$

For a certain RIN level σ, to make the oscillation amplitude decay by a factor of 1/e, we need the time $N_{1/e}$(in oscillation cycles) to be;

$$N_{1/e} = \frac{1.59}{\pi\sigma} \quad (68)$$

For two-photon Rabi oscillations ,When $\delta = \Delta_1 - \Delta_2 \gg |\Omega_1|, |\Omega_2|$, solving the Schrodinger equations gives the following approximate expression for the population on the Rydberg state $|r\rangle$, assuming initially $|c_g(0)|^2 = 1, |c_e(0)|^2 = |c_r(0)|^2 = 0$:

$$|c_r(t)|^2 = \sin^2(\frac{\Omega_R t}{2}) \quad (69)$$

Here $\Omega_R = \Omega_1\Omega_2/\delta$. This expression is also only true when $\Delta_+ = \Delta_1 + \Delta 2 + \frac{|\Omega_1|^2 - |\Omega_2|^2}{2\delta} = 0$ is satisfied. This condition guarantees a full population transfer between the ground state $|g\rangle$ and the Rydberg state$|r\rangle$.

When $\Delta_+ \neq 0$, expression (1) becomes:

$$|c_r(t)|^2 = \frac{\Omega_R^2}{\Omega'^2}\sin^2(\frac{\Omega' t}{2}) \quad (70)$$

where $\Omega'^2 = \Omega_R^2 + |\Delta_+|^2$.

In our following discussions, we always assueme that our noiseless system has $\Delta_+ = 0$.

If the two lasers driving the two-photon Rabi oscillations both have intensity noise:

$$\begin{aligned} I_1(t) &= I_{1_0} + \delta I_1(t) = I_{1_0}(1 + x_1(t)) \\ I_2(t) &= I_{2_0} + \delta I_2(t) = I_{2_0}(1 + x_2(t)) \end{aligned} \quad (71)$$

Assume that x_1 and x_2 both has normal distribution with 0 mean and variance σ_1^2 and σ_2^2:

$$f(x_i) = \frac{1}{\sqrt{2\pi}\sigma_i}e^{\frac{x_i^2}{2\sigma_i^2}} \quad (72)$$

where $i = 1, 2$.

Under this model, the modified Rabi rate Ω_i' will be:

$$\Omega_i' = \Omega_i\sqrt{1+x_i}, i = 1, 2 \quad (73)$$

Set $t_N = N\frac{2\pi}{\Omega_R}$, then the expected value of Rydberg state population can be calculated with the following integral, under the condition that $\Delta_+ = 0$:

$$\mathrm{E}[P_r] = \frac{1}{2\pi\sigma_1\sigma 2}\int_{-\infty}^{\infty}dx_1 \int_{-\infty}^{\infty}\sin^2(N\pi\sqrt{(1+x_1)(1+x_2)})e^{\frac{x_1^2}{2\sigma_1^2}}e^{\frac{x_2^2}{2\sigma_2^2}}dx_2 \quad (74)$$

Expanding the *sin* term in the integral to the second order, we get:

$$\sin^2(N\pi\sqrt{(1+x_1)(1+x_2)}) \approx \frac{N^2\pi^2x_1^2}{4} + \frac{N^2\pi^2x_2^2}{4} + \frac{N^2\pi^2x_1x_2}{2} \quad (75)$$

Putting this expansion back to the integral, we get an estimate for the expectation of occupancy, which is also the expected population error in Rabi oscillations:

$$\mathrm{E}[P_r] = \frac{N^2\pi^2\sigma_1^2}{4} + \frac{N^2\pi^2\sigma_2^2}{4} \quad (76)$$

B. frequency noise

Now we assume the laser's frequency drift is also Gaussian distributed. The frequency noise is defined as:

$$\Delta\nu = \nu - \nu_0 \quad (77)$$

where ν_0 is the unperturbed optical frequency. Define $x = 2\pi\Delta\nu/\Omega$, where Ω is the Rabi frequency for the two level system. Then the Gaussian distribution of x can be the following:

$$f(x) = \frac{1}{\sqrt{2\pi}\sigma}e^{-\frac{x^2}{2\sigma^2}} \quad (78)$$

Here $\Delta\nu_{rms} = x\sigma$ is the RMS value for frequency deviation.

For a two-level system resonant with laser frequency ν_0, the frequency noise will act as detunings. $\Delta = x\Omega$

The population for the excited state $|e\rangle$ in Rabi oscillations is:

$$P_e = \frac{\Omega^2}{\Omega^2+\Delta^2}\sin^2(\frac{\sqrt{\Omega^2+\Delta^2}t}{2}) \tag{79}$$

By plugging in $\Delta = x\Omega$ and $t = N\frac{2\pi}{\Omega}$ we get:

$$P_e = \frac{1}{1+x^2}\sin^2(N\pi\sqrt{1+x^2}) \tag{80}$$

The expected value of P_e will be the average over the distribution of x:

$$\mathrm{E}[P_e] = \frac{1}{\sqrt{2\pi}\sigma}\int_{-\infty}^{\infty}\frac{1}{1+x^2}\sin^2(N\pi\sqrt{1+x^2})e^{-\frac{x^2}{2\sigma^2}}dx \tag{81}$$

Then we can get expected value of P_g from the expression above:

$$\mathrm{E}[P_g] = \frac{1}{\sqrt{2\pi}\sigma}\int_{-\infty}^{\infty}[1-\frac{1}{1+x^2}\sin^2(N\pi\sqrt{1+x^2})]e^{-\frac{x^2}{2\sigma^2}}dx \tag{82}$$

We are going to discuss two special cases of N, where N are integers and half integers. In those cases we can simplify the expression for P_e and get an analytical expression for the error.

1. When N is integer, by doing Taylor expansion on the $\frac{1}{1+x^2}\sin^2(N\pi\sqrt{1+x})$ term to the fourth order, we can get the following approximation:

$$\frac{1}{1+x^2}\sin^2(N\pi\sqrt{1+x^2}) \approx \frac{N^2\pi^2x^4}{4} \tag{83}$$

The integral then becomes:

$$\mathrm{E}[P_e] = \frac{3N^2\pi^2\sigma^4}{4} \tag{84}$$

2. When N is half-integer, by doing Taylor expansion on the $\frac{1}{1+x^2}\sin^2(N\pi\sqrt{1+x})$ term to the second order, we can get the following:

$$1-\frac{1}{1+x^2}\sin^2(N\pi\sqrt{1+x^2}) \approx x^2 \tag{85}$$

The integral then becomes:

$$\mathrm{E}[P_g] = \sigma^2 \tag{86}$$

As a summary, if we start the Rabi oscillation at $P_g = 1$ when $t = 0$, the we have the following expression for errors:

$$\begin{cases}\mathrm{E}[P_g] = \sigma^2, & \text{N=0.5, 1.5, 2.5, 3.5,...}\\ \mathrm{E}[P_e] = \frac{3N^2\pi^2\sigma^4}{4}, & \text{N=1, 2, 3, 4,...}\end{cases}$$

Where $N = \frac{\Omega t}{2\pi}$, σ is defined as frequency deviation in terms of Rabi frequency $\sigma = 2\pi\Delta\nu_{rms}/\Omega$

In the case of band-limited white noise in the frequency noise spectrum, with bandwidth f_{max} and amplitude $FWHM/\pi$, where $FWHM$ is the linewidth of the corresponding lineshape in carrier domain, we have:

$$\sigma^2 = \frac{FWHMf_{max}}{\pi} \tag{87}$$

Then combining it with the expression for Rabi errors, we have:

$$\begin{cases}\mathrm{E}[P_g] = \frac{FWHMf_{max}}{\pi}, & \text{N=0.5, 1.5, 2.5, 3.5,...}\\ \mathrm{E}[P_e] = \frac{3N^2\pi^2FWHM^2f_{max}^2}{4}, & \text{N=1, 2, 3, 4,...}\end{cases}$$

For two photon Rabi oscillations,When there's frequency noise, then the term Δ_+ becomes a random variable which could be nonzero, and we need to find out its distribution. Assume that the frequency drift of each laser can be written as ξ_1 and ξ_2,as fig 2 shows, where $\xi_1 = \Delta_1^{'} - \Delta_1$, and $\xi_2 = \Delta_2^{'} - \Delta_2$.

We can now set up a model where ξ_i is measured by Ω_R:

$$\xi_i = x_i\Omega_R, i = 1,2 \tag{88}$$

Then similarly, we can assume that x_i has normal distribution with 0 mean and variance σ_i^2:

$$f(x_i) = \frac{1}{\sqrt{2\pi}\sigma_i}e^{\frac{x_i^2}{2\sigma_i^2}}, i = 1,2 \tag{89}$$

When the system doesn't have frequency noise, the term Δ_+ can be written as:

$$\Delta_+ = \Delta_1 + \Delta_2 + \frac{|\Omega_1|^2 - |\Omega_2|^2}{2(\Delta_1-\Delta_2)} \tag{90}$$

Then with frequency noise, it becomes:

$$\Delta_+^{'} = \Delta_1+\Delta_2+\Omega_R(x_1+x_2)+\frac{|\Omega_1|^2 - |\Omega_2|^2}{2(\Delta_1-\Delta_2)+2\Omega_R(x_1-x_2)} \tag{91}$$

Our purpose here is to study the distribution of the variable x_+, where it is defined as:

$$x_+ = \frac{\Delta_+^{'} - \Delta_+}{\Omega_R} \tag{92}$$

Then we can use the results in our single photon quasistaic frequency noise model, by replacing the term x in the single photon model by the term x_+. Here x_+ seems to represent the "equivalent" frequency drift for the two-photon system.

Combining equation (17) to (19), we get:

$$x_+ = x_1 + x_2 + \frac{1}{\Omega_R}[\frac{|\Omega_1|^2 - |\Omega_2|^2}{2(\Delta_1-\Delta_2)+2\Omega_R(x_1-x_2)} - \frac{|\Omega_1|^2 - |\Omega_2|^2}{2(\Delta_1-\Delta_2)}] \tag{93}$$

The third term in equation (20) has an general inverse-Gaussian distribution, which is also called Wald distribution, due to the $x_1 - x_2$ term on the denominator. Which is complicated and needs to be studied later.

Nonetheless, we can make an assumption that ξ_1 and ξ_2 are both much less than δ. Then equation(20) can be approximated to:

$$\begin{aligned} 3rdterm &= \frac{1}{\Omega_R}[\frac{|\Omega_1|^2 - |\Omega_2|^2}{2(\Delta_1 - \Delta_2) + 2\Omega_R(x_1 - x_2)} - \\ &\frac{|\Omega_1|^2 - |\Omega_2|^2}{2(\Delta_1 - \Delta_2)}] \\ &= \frac{1}{\Omega_R}[\frac{|\Omega_1|^2 - |\Omega_2|^2}{2(\Delta_1 - \Delta_2)}(1 - \frac{\Omega_R}{\delta}(x_1 - x_2)) - \\ &\frac{|\Omega_1|^2 - |\Omega_2|^2}{2(\Delta_1 - \Delta_2)}] \\ &= \frac{|\Omega_1|^2 - |\Omega_2|^2}{2\delta^2}(x_1 - x_2) \end{aligned} \tag{94}$$

This gives:

$$\begin{aligned} x_+ &= x_1 + x_2 + \frac{|\Omega_1|^2 - |\Omega_2|^2}{2\delta^2}(x_1 - x_2) \\ &= x_1 + x_2 + \alpha(x_1 - x_2) \end{aligned} \tag{95}$$

where $\alpha = \frac{|\Omega_1|^2 - |\Omega_2|^2}{2\delta^2}$.

We already know that x_1 and x_2 satisfies normal distribution, then using the properties of normal distributions, we get that x_+ also has normal distribution with zero mean, and a variance of:

$$\sigma_+^2 = (1+\alpha)^2\sigma_1^2 + (1-\alpha)^2\sigma_2^2 \tag{96}$$

Then we can transplant x_+ and σ_+ into the model that we developed for single photon(section 4.2 of note).

$$\mathrm{E}[P] = \frac{1}{\sqrt{2\pi}\sigma_+}\int_{-\infty}^{\infty}\frac{1}{1+x_+^2}\sin^2(N\pi\sqrt{1+x_+^2})e^{-\frac{x_+^2}{2\sigma_+^2}}dx \tag{97}$$

By doing Talor expansion on the sin^2 term, we can get an approximation for the integral:

$$\begin{cases} \mathrm{E}[P_g] = \sigma_+^2 + \frac{3N^2\pi^2\sigma_+^4}{4}, & \text{N=0.5, 1.5, 2.5, 3.5,...} \\ \mathrm{E}[P_e] = \frac{3N^2\pi^2\sigma_+^4}{4}, & \text{N=1, 2, 3, 4,...} \end{cases}$$

where $\sigma_+^2 = (1+\alpha)^2\sigma_1^2 + (1-\alpha)^2\sigma_2^2, \alpha$ is a constant, $\alpha = \frac{|\Omega_1|^2 - |\Omega_2|^2}{2\delta^2}$.

C. Comparison with numerical results one-photon transitions

In this section we are going to compare the results from the quasi-static model to the numerical results from the time-series simulations.

The noise we are simulating is a band-limit white frequency noise with a cut-off frequency F_c in its frequency domain. Before knowing the result, we assumed that the two results should match, espcially when the cut-off frequency F_c is low compared to the Rabi frequency Ω.

1. *Intensity Noise*

2. *Frequency Noise*

Simulations shows agreement between simulations and the quasi-static model numbers, where we are showing the errors from 8π and 9π rotations from both quasi-static model and numerical simulations, at different laser linewidths(lw).

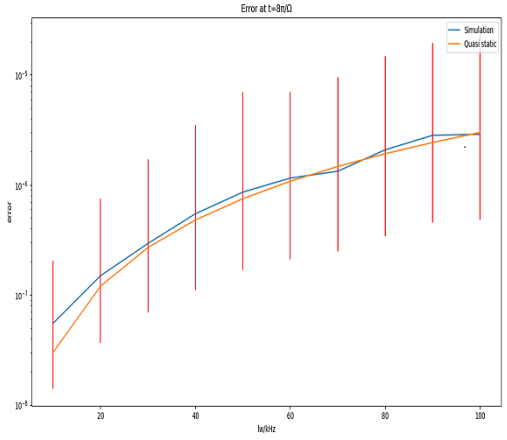

FIG. 3. Rabi Error with Frequency Noise for 8π pulse

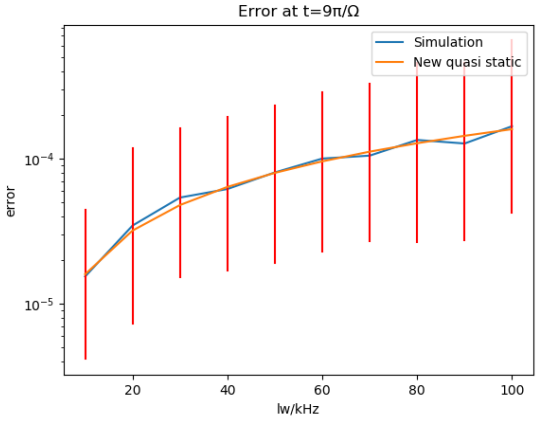

FIG. 4. Rabi Error with Frequency Noise for 9π pulse

D. Comparison with numerical results two-photon transitions

1. *Intensity noise*

2. *Frequency noise*

VI. DISCUSSION

How good does the laser have to be to achieve 10^{-3} or 10^{-4} gate errors?

[1] S. de Léséleuc, D. Barredo, V. Lienhard, A. Browaeys, and T. Lahaye, "Analysis of imperfections in the coherent optical excitation of single atoms to Rydberg states," Phys. Rev. A **97**, 053803 (2018).

[2] G. Di Domenico, S. Schilt, and P. Thomann, "Simple approach to the relation between laser frequency noise and laser line shape," Appl. Opt. **49**, 4801 (2010).

[3] D. S. Elliott, R. Roy, and S. J. Smith, "Extracavity laser band-shape and bandwidth modification," Phys. Rev. A **26**, 12 (1982).

[4] M. Zhu and J. L. Hall, "Stabilization of optical phase/frequency of a laser system: application to a commercial dye laser with an external stabilizer," J. Opt. Soc. Am. B **10**, 802 (1993).

[5] in *Frequency Standards* (John Wiley Sons, Ltd, 2003) https://onlinelibrary.wiley.com/doi/pdf/10.1002/3527605991.fmatter.

[6] P. Gallion and G. Debarge, "Quantum phase noise and field correlation in single frequency semiconductor laser systems," IEEE Journal of Quantum Electronics **20**, 343–349 (1984).

[7] L. Richter, H. Mandelberg, M. Kruger, and P. McGrath, "Linewidth determination from self-heterodyne measurements with subcoherence delay times," IEEE Journal of Quantum Electronics **22**, 2070–2074 (1986).